Eur. Phys. J. B **34**, 421–428 (2003)
DOI: 10.1140/epjb/e2003-00240-2

THE EUROPEAN PHYSICAL JOURNAL B

Electrical resistivity of the Ti_4O_7 Magneli phase under high pressure

C. Acha[1,a], M. Monteverde[1,2,b], M. Núñez-Regueiro[2], A. Kuhn[3], and M.A. Alario Franco[4]

[1] Laboratorio de Bajas Temperaturas, Departamento de Física, FCEyN, Universidad de Buenos Aires, Pabellón I, Ciudad Universitaria, 1428 Buenos Aires, Argentina
[2] CRTBT, CNRS, BP166, 38042 Grenoble Cedex 09, France
[3] Facultad de Ciencias Experimentales y Técnicas, Universidad San Pablo, 28668 Boadilla del Monte, Spain
[4] Facultad de Ciencias Químicas, Universidad Complutense, 28040 Madrid, Spain

Received 11 February 2003 / Received in final form 19 June 2003
Published online 9 September 2003 –

Abstract. We have measured resistivity as a function of temperature and pressure of Ti_4O_7 twinned crystals using different contact configurations. Pressures over 4 kbar depress the localization of bipolarons and allow the study of the electrical conduction of the bipolaronic phase down to low temperatures. For pressures $P > 40$ kbar the bipolaron formation transition is suppressed and a nearly pressure independent behavior is obtained for the resistivity. We observed an anisotropic conduction. When current is injected parallel to the principal axis, a metallic conduction with interacting carrier effects is predominant. A superconducting state was not obtained down to 1.2 K, although evidences of the proximity of a quantum critical point were noticed. While when current is injected non-parallel to the crystal's principal axis, we obtained a logarithmic divergence of the resistivity at low temperatures. For this case, our results for the high pressure regime can be interpreted in the framework of interacting carriers (polarons or bipolarons) scattered by Two Level Systems.

PACS. 71.10.Ay Fermi-liquid theory and other phenomenological models – 71.30.+h Metal-insulator transitions and other electronic transitions – 72.10.-d Theory of electronic transport; scattering mechanisms

1 Introduction

The study of electronic properties in metals which their charge carriers could be associated with bipolarons has recently raised some interesting discussions in the quest to determine the microscopic origin of high T_c superconductivity [1–3]. Alexandrov and Mott [4] had claimed that many of the experimental properties of high temperature superconductors can be explained considering a Bose condensation of their bipolaronic charge carriers. Chakraverty *et al.* [1] argue that the condensation temperature for this type of bosonic superconductors can not be much higher than 10 K. The possibility of a superconductivity related to bipolarons was previously studied theoretically by several authors [5–7], but up to now there is not a clear experimental proof of the existence of a superconducting state based on a Bose condensation of bipolarons.

On the other hand, characteristic transport properties of a bipolaronic metal are not well established experimentally. Theoretical studies [8] asserted a logarithmic divergence of the resistivity at low temperatures, in the case of bipolaronic carriers scattered by shallow potential wells related to disorder. This type of divergence was particularly observed in the anisotropic low-temperature normal-state resistivity of underdoped $La_{2-x}Sr_xCuO_4$ single crystals, where superconductivity was suppressed with a 60 T pulsed magnetic field [9,10].

In order to contribute to this debate and to gain some insight in transport properties related to (bi)polaron diffusion, we considered the study of a material with a conduction related to these quasi-particles. The low temperature electrical conduction of the Ti_4O_7 Magneli phase can be assign to bipolaron diffusion as was revealed by electrical resistivity, magnetic susceptibility, specific heat, ESR and crystal structure studies [11–16]. This compound shows metal-non metal transitions (3 phases and 2 resistive transitions, with related specific heat jumps) which are probably associated to the fact that it has one $3d$ electron per two cation sites, and two valence states for the Ti (3+ and 4+). The crystal structure of Ti_4O_7, shown in Figure 1 , is built up by infinite (TiO_6) octahedra in two dimensions, forming a rutile slab, having a finite width of n octahedra along the C crystallographic direction. The slabs are delimited by the shear planes, referred as the

[a] Also fellow of CONICET of Argentina
e-mail: acha@df.uba.ar
[b] Scholarship from CONICET of Argentina

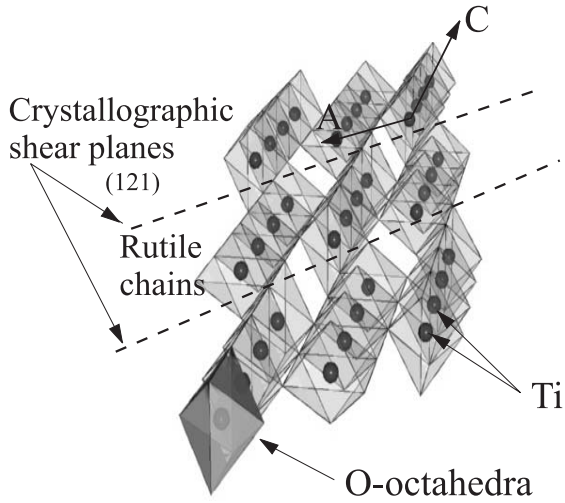

Fig. 1. Crystal structure of Ti_4O_7. This structure is formed by successive rutile blocks (TiO_2), infinite in 2 dimensions and of 4 octahedra width along the C axis, bounded by the crystallographic shear planes, corresponding to the (121) planes referred to the rutile structure.

(121) planes of the rutile structure. The octahedra share corners, faces or borders, determining 4 different crystallographic sites for the Ti.

For the low temperature phase (LTP) ($T \leq T_{bl}$, with $T_{bl} \simeq 130$ K (on cooling) or 140 K (on heating) being the bipolaron localization temperature) an insulator behavior is found, where the Ti^{3+} are well localized in chains of Ti^{3+}-Ti^{3+} pairs, forming a non magnetic bond and creating a local distortion of the lattice. This pair, stabilized by the lattice deformation is known as a bipolaron [17]. For the intermediate temperature phase (ITP) ($T_{bl} < T \leq T_{bf}$, with $T_{bf} \simeq 150$ K, being the bipolaron formation temperature) bipolarons become thermally diffused and there is a correlative increase of the electrical conduction. In the high temperature phase (HTP) ($T > T_{bf}$), the 3d electrons become delocalized; a sudden increase of the magnetic susceptibility (Pauli paramagnetism) is observed while the conduction becomes metallic [15].

It was tempting to extend towards lower temperatures the existence window of the ITP. On one hand, to favor the conditions for a possible bipolaron condensation that would yield a superconducting state. On the other hand, the study of transport properties of such a material can reveal new features, besides the ones that were predicted theoretically [8] but not confirmed experimentally.

V impurities were previously introduced for this purpose [14,15,18]. They create local structural distortions which generate long range interactions that stabilize the ITP. Indeed, the Ti^{3+} - Ti^{3+} distance is lower in the V doped sample and the temperature of the metal-insulator transition is depressed. Unfortunately this induces at the same time the increase of the background disorder which produces a glassy conduction.

By applying an external pressure, structural distortions can be generated in order to extend the IT phase, but without the disadvantage of introducing impurities. In accordance to this, it was shown that the formation and localization of bipolarons can be both depressed applying pressures up to 40 kbar [19]. The rate of depression of the localization temperature is higher than the formation one. The temperature width for bipolaron diffusion is then enhanced and their transport properties can be studied down to low temperatures.

In this paper we report DC resistivity measurements (R) as a function of temperature (T) and pressure (P) of Ti_4O_7 twinned crystals, for 4 K $< T <$ 300 K and P up to 220 kbar. An anisotropic electrical transport was observed and analyzed for the whole pressure regime. Pressure depress the localization and the formation transitions yielding to a conducting regime down to low temperatures. A metallic behavior with interacting carriers effects and signs of the proximity of a quantum critical point is obtained when current is applied parallel to the principal axis of crystals, while a logarithmic divergence on the resistivity on decreasing temperature is observed for currents applied with components in a perpendicular direction.

2 Experimental

Ti_4O_7 powder was made by heating finely ground mixtures of TiO_2 (rutile) and Ti metal in an evacuated silica tube at 1150 C during one week, as previously described [20]. Small single crystals ($0.1 \times 0.1 \times 0.3$ to 0.6 mm^3) could be extracted from these powders. Bigger twinned crystals ($1 \times 1 \times 3$ mm^3) were obtained by a chemical transport reaction using Iodine as a transport agent. For this, about 1g of freshly prepared Ti_4O_7 powder and 0.1 g of iodine were introduced in a silica tube, which was then sealed under vacuum. The tube was placed in an horizontal furnace and heated to 950 °C during two weeks. The tube charge was held in the hottest zone, and some well formed, blue-black crystals were deposited in a colder region.

X-ray powder diffraction experiments were conducted to check the purity of the obtained material. A Siemens Kristalloflex D-5000 diffractometer operating with CuK alpha radiation at a scan rate of 0.1 degrees/min was used. Single crystal X-ray diffraction experiments were performed on several as-grown specimens. The crystals were stucked on a glass capillary and mounted in a four-cycle Enraf-Nonius CAD4 diffractometer. The diffraction data were collected using the $2\theta\omega$ scan method with a scan rate of 1 degree/min at room temperature. The diffractometer was operated at 40 kV/20 mA; a graphite - monochromatized MoK alpha beam ($\lambda = 0.71069$) was used.

Samples were also characterized at ambient pressure by measuring their ac susceptibility as a function of temperature. Using a mutual inductance bridge, with an excitation signal frequency of 119 Hz, and 1 Oe of magnetic field amplitude, an overall sensitivity of 10^{-8} emu can be attained.

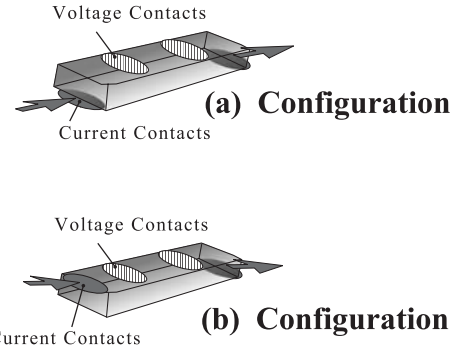

Fig. 2. Contact configurations used to measure the resistance of the samples.

Resistivity under high pressure was measured using a hydrostatic and a quasi-hydrostatic experimental setup depending on the pressure range focused. For pressures bellow 10 kbar, a hydrostatic piston cylinder self-clamped cell was used, while for higher pressures, starting from 15 kbar and up to 220 kbar, we applied the Bridgman configuration with sintered diamond anvils. In the former case, a 50-50 mixture of kerosene and transformer oil was used as the pressure transmitting medium and manganine as a manometer. In the latter case, pyrophillite was used as a gasket and steatite as the pressure medium that favors quasi-hydrostatic conditions. Lead was used inside the cell as a manometer by monitoring its superconducting transition temperature. The pressure gradient was estimated from the width of this transition and corresponds to a 5−10% of the applied pressure, for pressures $\leq$ 100 kbar, and saturates at a maximum value of 10 kbar for higher pressures. We use a conventional 4 terminal DC technique to measure resistivity under high pressure at different temperatures. Electrical contacts were made using thin Pt wires, fixed to the sample using silver paste for the hydrostatic cell, and solely by pressure for the Bridgman setup.

We have measured over 8 different parallelepiped twinned crystals of typical dimensions $0.1 \times 0.1 \times 0.6$ mm^3 under high pressure, which have given clearly reproducible results. Depending on crystal, the electrical current was applied parallel (a) or non-parallel (b) to its principal axis. These different contact configurations are represented in Figure 2. They were initially chosen for the high pressure cell setup convenience. Due to the large contact size respect to the small dimensions of the crystals, it was meaningless to modify our contact setup in order to apply the Montgomery method [21] for a satisfactory determination of the anisotropic resistivities. Although the obtained estimated resistivity values are within the range of those previously reported [13,15,22], they only correspond to effective values, computed considering the conducting area perpendicular to the principal axis direction, for the (a) and (b) configurations. From the structural point of view, according to a previous work [22], Ti_4O_7 crystals have their longest dimension along the B crystallographic axis and show a metallic like conductivity at room temperature. According to this, the (a) contact configuration should be testing essentially the conduction along the B crystal direction, while the (b) configuration must include conductivity contributions of other crystallographic directions. Nevertheless, by simulating an anisotropic resistance network, we also checked that effectively the particular resistivity dependencies with temperature obtained were not just a consequence of the variation of the anisotropic resistivity ratio with temperature. Thus, our approach, albeit certainly inexact, still remains as an effective way of determining the general temperature behavior of the resistivity of these small and anisotropic samples under high pressure.

3 Results

We have analyzed the X-ray diffraction powder patterns in order to study the structure of the samples. The refined cell parameters and angles of the triclinic unit cell (space group A-1) agree well with literature values [23]. Lattice parameters were determined for small single crystals by least-squares refinement of the 2θ values of 25 very well-centered strong reflections between 20 and 45 degrees. Cell parameters and angles of the unit cell obtained for all crystals were analogous with those expected for Ti_4O_7.

Samples measured using the (a) contact configuration show a metallic behavior at room temperature and a resistivity at ambient pressure of $\simeq$ 2 mΩcm, while using the (b) contact configurations they display a semiconducting-like dependence and a resistivity of $\simeq$ 10 mΩcm. They develop the bipolaronic transitions, with a 77 K to 300 K resistivity ratio at ambient pressure of $\simeq 10^8$ and $\simeq 10^6$ depending on the contact configuration. These different values and dependencies for the resistivity of Ti_4O_7 can be observed comparing the data of previous papers [13,15], and have been interpreted as an intrinsic electrical transport property related to the anisotropic conduction of this material [24].

Considering our experimental sensitivity of 10^{-8} emu for the ac susceptibility, various small Ti_4O_7 crystals were assembled together in order to detect their small signal change when they undergo the bipolaron formation transition at T_{bf}. Despite the poor signal to noise ratio obtained, the measured ac susceptibility, presented in Figure 3, shows effectively a sudden reduction at $T_{bf} \sim 150$ K and a small value for lower temperatures, in accordance with previous results [13].

In Figures 4 and 5 we can see $\rho(T)$ at different applied pressures (P) for the (a) and (b) configurations, respectively. Both transition temperatures (T_{bf} and T_{bl}) decrease with increasing pressure, although the T_{bl} transition can be seen only in the hydrostatic pressure setup as it is steeply decreased by a small pressure ($T_{bl} \to 0$ for $P \simeq 4$ kbar).

The localization transition temperature (T_{bl}) shows an hysteretical behavior (not shown for clarity) which is consistent with the one previously reported [13,14]. A remanence of the metallic state can be noticed in the low temperature range of the data of Figure 5 as a positive $\mathrm{d}\rho/\mathrm{d}T$.

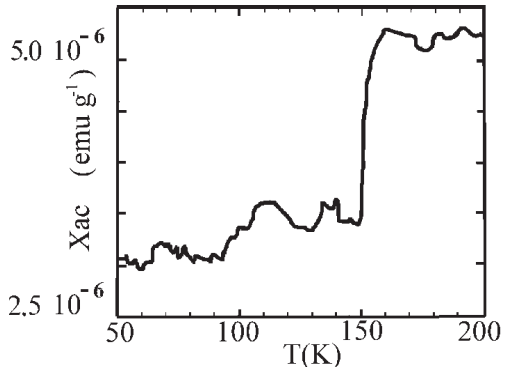

Fig. 3. ac susceptibility of Ti_4O_7 as a function of temperature at ambient pressure. A sudden reduction of the Pauli susceptibility can be seen for temperatures bellow $T_{bf} \simeq 150$ K.

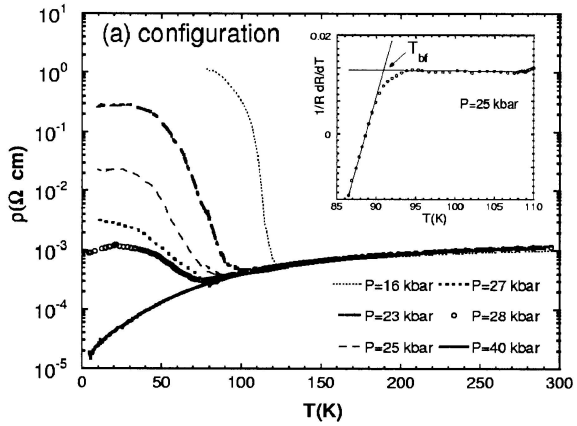

Fig. 4. Resistivity as a function of temperature of Ti_4O_7 in the (a) configuration for different pressures (cooling). In the inset the criteria to define T_{bf} is presented. In this pressure range, only the transition at T_{bf} can be observed as the temperature of the bipolaron localized phase (T_{bl}) was abruptly reduced by pressure.

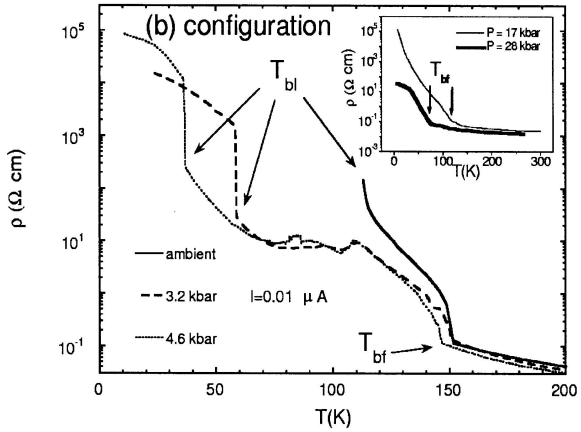

Fig. 5. Resistivity as a function of temperature of Ti_4O_7 in the (b) configuration for different pressures (cooling). The inset displays the resistivity behavior for a higher pressure regime, where the bipolaron localization transition at T_{bl} is no longer present down to our minimum experimental temperatures.

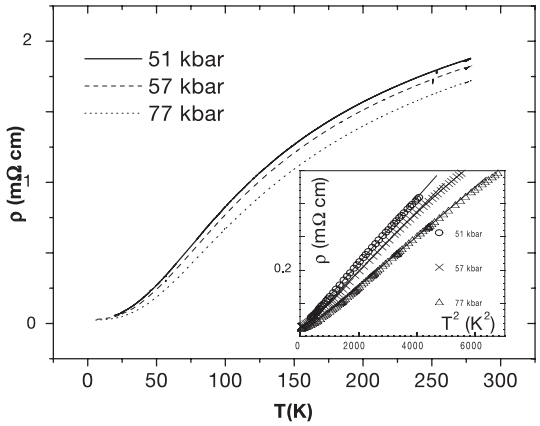

Fig. 6. Resistivity for the high pressure regime ($P \geq 40$ kbar), in the (a) contact configuration. The inset shows that resistivity can be represented, approximately by a T^2 law at low temperatures.

Now, if we focus our attention on the (a) configuration results (shown in Fig. 6), we observe a poor metallic conduction for pressures $P \geq 38$ kbar (~ 2 mΩcm at room temperature), similar to those observed for other transition-metal oxides [25,26]. The high temperature behavior is sublinear while the low temperature resistivity shows some signs of interacting carriers effects, as can be noticed in the inset of Figure 6 as an approximate T^2 dependence of the resistivity. Evidences of a superconducting transition were not observed down to 1.2 K over this pressure range. For temperatures lower than ~ 4 K a residual resistivity $\rho_0 \sim 20$–60 $\mu\Omega$ cm is obtained, which is reduced with increasing pressure.

Taking into account the possible proximity of a quantum critical point (QCP) [27], induced by the fact that T_{bf}, which defines a paramagnetic metallic to nonmagnetic insulator transition, probably tends to 0 for a critical pressure P_c in the 34–37 kbar range, we evaluated the coefficient A and the exponent N of the resistivity expression $\rho = \rho_0 + AT^N$ as a function of pressure. For each pressure, a constant N value is obtained for temperatures in the range 2 K $\leq T \leq$ 40 K. Results are displayed in Figure 7 and in Figure 8.

For $P \rightarrow 34-37$ kbar a divergence of the A parameter and the exponent $N < 2$ are observed. With increasing pressure, the N value increases, probably related to the relative increase of the phonon contribution to the electronic scattering determined by the A coefficient diminution over one order of magnitude.

In Figure 9 we show our results using the (b) contact configuration. A very poor conduction is observed ($10-100$ mΩ cm, probably depending on sample's twins and on current density, as it will be shown later) with a low P dependent behavior for pressures up to 230 kbar. Below 40 K a Ln(1/T) dependence is observed, with a saturation regime at low temperatures. Both the saturation resistance and the logarithmic slope decrease with increasing pressure. A non-ohmic behavior was also detected in this region (see Fig. 12), but these studies will be published elsewhere.

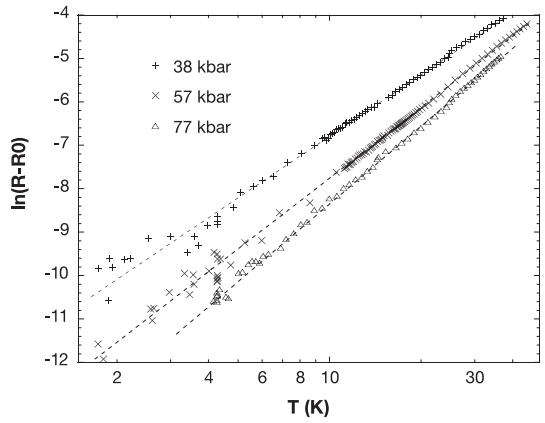

Fig. 7. The logarithm of ρ-ρ_0 is plotted *vs.* T for different pressures. The dashed lines were calculated according to the expression $\rho = \rho_0 + AT^N$.

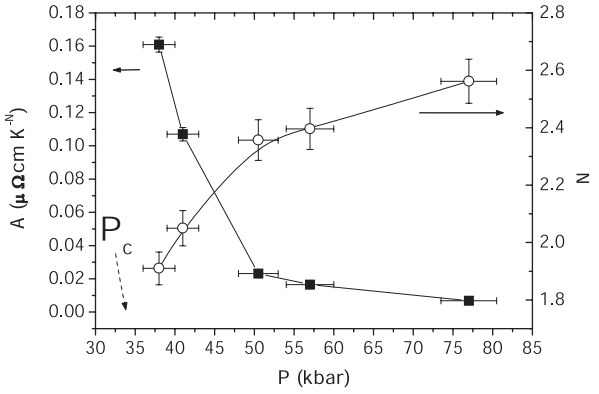

Fig. 8. The A and N parameters determined by a fit of the data shown in Figure 7 to $\rho = \rho_0 + AT^N$ as a function of pressure for 10 K $\leq T \leq$ 40 K.

Although our crystals are twinned, their electrical transport characteristics were strictly determined by the chosen current configuration setup ((a) or (b)). As a consequence, this indicates a particular correlation in the growing directions of twins in these crystals. Considering this, the resistivity shown for the (a) configuration should be essentially related to a mean value of the metallic resistivity tensor in the B axis direction, while the semiconducting-like resistivity related to the (b) configuration should be dominated by the resistivity tensor in the C crystallographic direction, where the shear planes must act as a source of additional scattering.

4 Discussion

Pressure modifies bipolaron ordering (localization) and formation transition temperatures (T_{bl} and T_{bf}) in a similar way as V incorporation does in the $(Ti_{1-x}V_x)_4O_7$ compound [15]. A phase diagram, shown in Figure 10, was drawn including the electrical transport characteristics observed for the (a) and (b) contact arrangement, where the T_{bl} transition was measured when cooling the sample. For

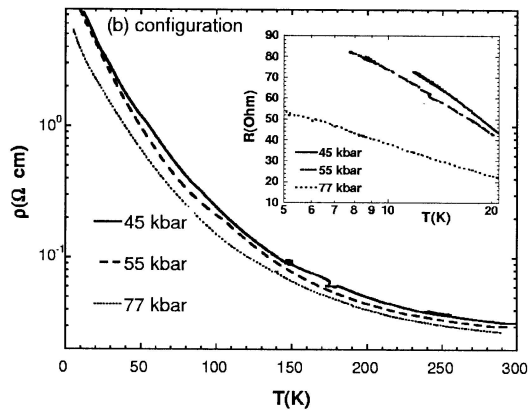

Fig. 9. Temperature dependence of the resistivity at different pressures in the (b) contact configuration for a pressure regime where the transitions are no longer seen down to our minimum experimental temperatures. The inset shows a logarithmic behavior at low temperatures.

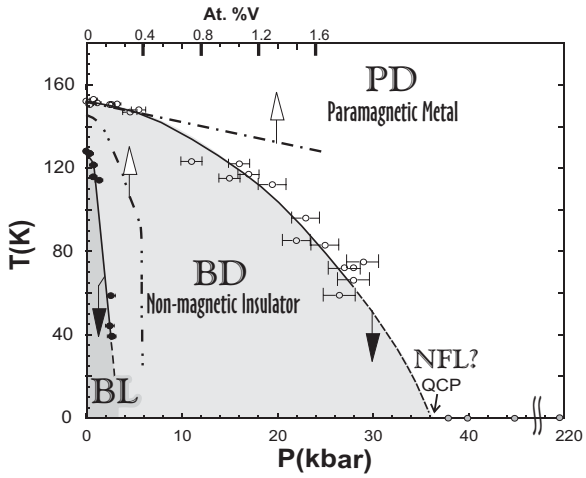

Fig. 10. The phase diagram shows the pressure dependence of (○) the bipolaron formation (T_{bf}) and (●) localization (T_{bl}) transition temperatures. For comparison, the dot-dashed curves show both transition temperatures for the V-doped samples. BL: bipolaron localization. BD: bipolaron diffusion. PD: polaron diffusion. NFL: non-Fermi liquid. QCP: quantum critical point.

comparison, results of the V-doped samples are also plotted but, in this case, the T_{bl} transition was determined by heating the sample. To do so, an arbitrarily empirical scaling was established between the V content and the applied pressure, as was determined for other systems [28], forcing the V linear dependence of the bipolaron formation temperature, T_{bf}(%V), to match the linear $T_{bf}(P)$ dependency for low pressures ($P \leq 5$ kbar).

Although the similarity of the results is probably based on the fact that both V incorporation and pressure decrease the Ti-Ti distance, generating a local chemical compression of the structure, there are some clear differences. The effect of pressure on band structure and lattice modes seems to be more significant than rigid band filling and impurities centers for the appearance and ordering of

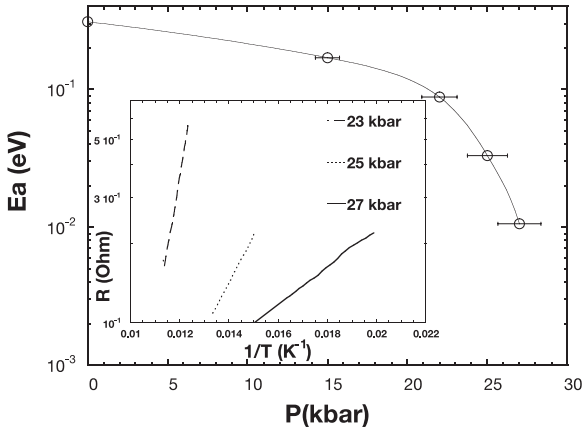

Fig. 11. Pressure dependence of the activation energy E_a for the resistivity of the ITP. The inset shows an Arhenius plot for the resistivity at different pressures.

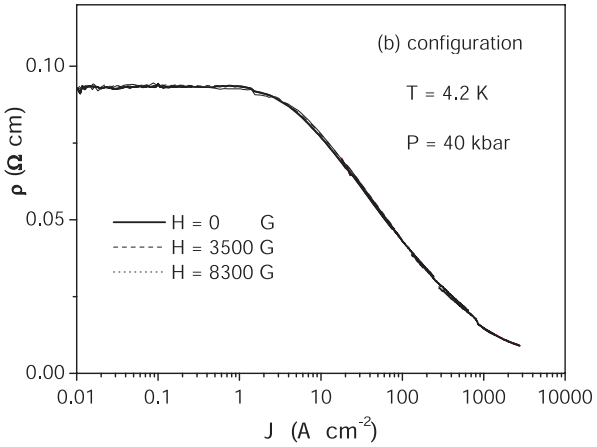

Fig. 12. Magnetic field sensitivity of the current dependent resistivity at low temperatures in the (b) contact configuration. Within our experimental resolution, no appreciable magnetic effects are observed.

bipolarons: The decrease and suppression of T_{bl} is more pronounced by applying an external pressure than by V incorporation. This also states for T_{bf} in the case of pressures $P > 5$ kbar. Besides, when T_{bl} vanishes by the V-generated structural distortions, T_{bf} is smoothly reduced to ~ 145 K. Contrary to this, pressure decreases T_{bf} down to ~ 60 K, where it become difficult to distinguish the associated resistive change. This is due to the fact that the activation energy, E_a, that characterizes the electrical conduction of this intermediate phase, is steeply reduced by pressure, as it can be seen in Figure 11.

As E_a is expected to be the hopping energy of the bipolarons, which is assumed to be half their binding energy [12,18], this pressure-induced sheer drop of E_a is indicating an excess of conduction probably related to hopping of single polarons. Within this picture, pressure reduces the binding energy of bipolarons yielding to an electrical conduction mediated by bipolarons and by single thermally excited polarons. In this context, the metallic behavior observed in Figure 5 at low temperatures can be associated with the coexistence of the high temperature paramagnetic metallic phase and the low temperature bipolaronic insulator. For small pressures, this phase separation can be related to the existence of small metallic regions where the bipolaronic transition is not favored, probably as a consequence of local structural distortions which inhibit the formation of bipolarons. As pressure increases, the decrease of E_a no longer favors the binding of bipolarons, leading to an increasing metallic conduction.

4.1 (a) Contact configuration

The approximated T^2 dependence of the resistivity in the (a) contact configuration for pressures $P \geq 40$ kbar (see the inset of Fig. 6) reveals a large T^2 term which is consistent with a picture of a highly correlated electron liquid. A rough estimation of the γ coefficient of the electronic specific heat can be done considering the empirical relationship between the A and the γ parameter established by Kadowaki and Woods [29]. A $\gamma \simeq 100$ mJ/(mol K^2) ($P = 40$ kbar, $N = 2$) points out the magnitude of the electron-electron interaction. The strong enhancement of the A quantity would then be correlated with the approach to the metal-insulator transition developed at T_{bf}. For the temperature range considered, electron-phonon contributions can not be minimized and the N parameter can be a mean value fixed by the weighted contributions of the electron-phonon and the electron-electron scatterings. The increase of the N value with increasing pressure can then be assigned to the reduction of the electron-electron contribution suggested by the diminution of the A parameter.

Nevertheless more detailed measurements are needed near the possible critical pressure P_c to determine if the divergence of the A parameter and, more important, the tendency to have an $N < 2$ are evidences that are suggesting a non-Fermi liquid behavior (NFL), instead of the proximity of a metal-insulator transition. Then, this possible NFL behavior would be probably related to the vicinity of a QCP [30] for a critical pressure P_c in the 34−37 kbar range. The QCP can be associated to the fact that $T_{bf}(P_c) = 0$ K, setting up a phase transition between a non-magnetic (bipolaronic-insulator) and a Pauli paramagnetic (polaronic-metal) material at $T = 0$ K. A similar behavior was observed in $BaVS_3$ under pressure [31].

4.2 (b) Contact configuration

An interpretation of our results obtained for the (b) contact configuration must consider the logarithmic divergence when decreasing temperature.

A logarithmic divergence in the resistivity can be found in dilute magnetic alloys, or Kondo systems, where the conduction electrons are scattered with magnetic impurities. Our Ti_4O_7 samples are clearly not a Kondo system, as magnetic impurities are not supposed to be present, as was confirmed by its low paramagnetic susceptibility at low temperatures, shown in Figure 3. Moreover, no appreciable magnetic field effects on the resistivity were

observed, as it is shown in Figure 12, contrary to what we will expect for a Kondo system.

The logarithmic temperature dependence of the resistivity can also led us to consider the framework used to describe electrical conduction in 2D systems [32], although, from the structural point of view, the oxygen octahedra chains form a 3D interconnected network, so that a bidimensional behavior can not be necessarily expected. In the case of a 2D conduction, a magnetic field dependence of the resistivity should be obtained, which was not observed experimentally as it is shown in Figure 12, although higher magnetic field are necessary to obtain a conclusive result. Also, to our knowledge, there are not bulk samples that show an electric conduction characteristic of localized 2D systems.

As the presence of bipolaronic carriers in the high pressure phase of Ti_4O_7 ($P \geq 40$ kbar) can not be completely rejected, we can also consider that the logarithmic divergence observed in the (b) contact configuration can be related to a diffusion of bipolarons, scattered by random shallow potential wells [8] in that particular direction. This disorder can be generated by oxygen vacancies or by the intergrowth of another members of the series Ti_nO_{2n-1} which usually occurs along the crystallographic C axis [16]. In this case, resistivity can be expressed at low temperatures (neglecting localization effects) by the following equation:

$$\rho(T) \simeq B\mathrm{Ln}\left(\frac{E_0}{k_B T}\right) \tag{1}$$

where B is a constant, $E_0 = \pi^4\hbar^2 \ / \ 128 \ \mathrm{m}_B \ \mathrm{a}_{min}^2$, m_B is the bipolaronic mass and a_{min} is the minimum size of the distribution of potential wells, which should be near the interatomic spacing. The decrease of the logarithmic slope with pressure (see the inset of Fig. 9) can be interpreted, within this theoretical approach, as a reduction of the product $\mathrm{a}_{min}^2 \ \mathrm{m}_B$, which is consistent with a pressure-induced reduction of the interatomic spacing and of the electron-phonon coupling which produces a decrease of the bipolaron's mass.

Another possible interpretation of the observed logarithmic divergence in the resistivity at low temperatures is related to the electrical conduction in many metallic glasses [33,34], where it is assumed that the conduction electrons interact with atoms placed in a double potential well, which can tunnel from one position to the other. This tunneling between the two state configurations or two level systems (TLS), which may be assisted by the electrons, generates a new source of scattering for the conduction process. This effect is usually not sensitive to the application of a magnetic field, unlike for the Kondo alloys. Resistivity can be described by the following empirical expression:

$$\rho(T_{eff}) = C[1 - D\mathrm{Ln}(T_{eff})] \tag{2}$$

where

$$T_{eff}^2 = T^2 + \left(\frac{\Delta}{k_B}\right)^2 \tag{3}$$

Δ is the TLS energy separation and C and D are suitable constants.

Although this model was initially criticized [35,36] as it predict a contribution to the resistivity one order of magnitude less than the experimental one, further investigations opened the possibility of an incremental effect of this contribution when many body problems are taken into account [37].

The microscopic origin of TLS in Ti_4O_7 can be possibly related to the different Ti site occupancy at low temperatures, or to the dynamic equilibrium between two superstructures, revealed in previous studies [16]. Also, it had been shown that paired-electrons behave as TLS at low temperatures [38,39]. There is no obvious theoretical distinction between the motion of electrons accompanied by local displacements of ions and the atomic motion proposed in the tunneling model, so that the origin of the TLS can be intrinsically related to bipolaronic diffusion.

5 Conclusions

An anisotropic electrical conduction with particular features was revealed using different contact arrangements in Ti_4O_7 twinned crystals under high pressure. Although a superconducting state was not achieved down to our minimum experimental temperatures, a rich phase diagram was obtained, as shown in Figure 10. Both formation and localization transition temperatures are depressed increasing pressure. The possible proximity of a pressure-induced QCP was established in the metallic-like conduction contact arrangement, as well as a conducting regime with clear signs of a highly correlated electron liquid, for pressures over 40 kbar. A logarithmic divergence in the resistivity with decreasing temperature was observed using the non-parallel contact setup ((b) contact configuration). In this latter case, a valid explanation of the transport characteristics observed for the whole temperature range studied seems to be closely related to an electrical transport based on polarons (or excited bipolarons) scattered by TLS.

This work was partially supported by CONICET of Argentina (PEI 146/98) and Fundación Antorchas (A-13462/1). We also are indebted to J. Lorenzana, P. Lee, J. Souletie and M. Rozenberg for fruitful discussions. We also acknowledge technical assistance from C. Chiliotte, D. Giménez, E. Pérez Wodtke and D. Rodríguez Melgarejo.

References

1. B.K. Chakraverty, J. Ranninger, D. Feinberg, Phys. Rev. Lett. **81**, 433 (1998)
2. A.S. Alexandrov, Phys. Rev. Lett. **82**, 2620 (1999)
3. B.K. Chakraverty, J. Ranninger, D. Feinberg, Phys. Rev. Lett. **82**, 2621 (1999)
4. A.S. Alexandrov, N.F. Mott, *High Temperature Superconductors and Other Superfluids* (Taylor & Francis, London, 1994)

5. A.S. Alexandrov, J. Ranninger, Phys. Rev. B **23**, 1796 (1981)
6. E. Iguchi, T. Yamamoto, R.J.D. Tilley, J. Phys. Chem. Solids **49**, 205 (1988)
7. R. Micnas, J. Ranninger, S. Robaszkiewicz, Rev. Mod. Phys. **62**, 113 (1990)
8. A.S. Alexandrov, Phys. Lett. A **236**, 132 (1997)
9. Y. Ando *et al.*, Phys. Rev. Lett. **75**, 4662 (1995)
10. Y. Ando *et al.*, J. Low Temp. Phys. **105**, 867 (1996)
11. C. Schlenker, S. Lakkis, J.M.D. Coey, M. Marezio, Phys. Rev. Lett. **23**, 1318 (1974)
12. B.K. Chakraverty, C. Schlenker, J. Phys. Colloq. France **37**, C4-353 (1976)
13. S. Lakkis, C. Schlenker, B.K. Chakraverty, R. Buder, Phys. Rev. B **14**, 1429 (1976)
14. C. Schlenker, S. Ahmed, R. Buder, M. Gourmala, J. Phys. C **12**, 3503 (1979)
15. C. Schlenker, M. Marezio, Phil. Mag. B **42**, 453 (1980)
16. Y.L. Page, M. Marezio, J. Solid State Chem. **53**, 13 (1984)
17. P.W. Anderson, Phys. Rev. Lett. **34**, 953 (1975)
18. C. Schlenker, in *Bipolarons in transition metal oxides*, *Physics of disordered materials*, edited by D. Adler, H. Fritzsche, S.R. Ovschinsky (Plenum Press, NY, 1983), pp. 369−389
19. C. Acha, M. Núnez-Regueiro, M.A.A. Franco, J. Souletie, Czech. J. Phys. **46**, 2681 (1996)
20. S. Andersson, B. Collen, U. Kuylenstierna, M. Magneli, Acta Chem. Scand. **11**, 1641 (1959)
21. H.C. Montgomery, J. Appl. Phys. **42**, 2971 (1971)
22. R.F. Bartholomew, D.R. Frankl, Phys. Rev. **187**, 828 (1969)
23. S. Andersson *et al.*, Acta Chem. Scand. **13**, 989 (1959)
24. A.D. Inglis, Y.L. Page, P. Strobel, C.M. Hurd, Solid State Phys. **16**, 317 (1983)
25. D.B. McWhan, T.M. Rice, Phys. Rev. Lett. **22**, 887 (1969)
26. N.F. Mott, *Metal-Insulator Transitions* (Taylor & Francis, London, 1997)
27. S.L. Sondhi, S.M. Girvin, J.P. Carini, D. Shahar, Rev. Mod. Phys. **69**, 315 (1997)
28. D.B. McWhan *et al.*, Phys. Rev. B **7**, 1920 (1973)
29. K. Kadowaki, S.B. Woods, Solid State Commun. **58**, 507 (1986)
30. T. Moriya, T. Takimoto, J. Phys. Soc. Jpn **64**, 960 (1995)
31. L. Forró *et al.*, Phys. Rev. Lett. **85**, 1938 (2000)
32. P.A. Lee, T.V. Ramakrishnan, Rev. Mod. Phys. **57**, 287 (1985)
33. R.W. Cochrane, R. Harris, J.O. Strom-Olson, M.J. Zuckermann, Phys. Rev. Lett. **35**, 676 (1975)
34. R. Harris, J.O. Strom-Olsen, in *Glassy Metals II*, No. 53 in *Topics in Applied Physics*, edited by H. Beck, H.J. Guntherodt (Springer-Verlag, NY, 1983), pp. 325–342
35. J.L. Black, B.L. Gyorffy, Phys. Rev. Lett. **41**, 1595 (1978)
36. J.L. Black, B.L. Gyorffy, J. Jackle, Philos. Mag. **40**, 331 (1979)
37. J.L. Black, in *Glassy Metals I*, No. 46 in *Topics in Applied Physics*, edited by H. Beck, H.J. Guntherodt (Springer-Verlag, NY, 1981), p. 167
38. D.L. Fox, B. Golding, W.H. Haemmerle, Phys. Rev. Lett. **49**, 1356 (1982)
39. W.A. Phillips, Rep. Prog. Phys. **50**, 1657 (1987)